Trifluoromethylaryl-Substituted Quinoxalines: Unusual Ruthenium-Amidininate Complexes and their Suitability for Anellation Reactions

Frank Schramm[a], Dirk Walther[a], Helmar Görls[a], Christian Käpplinger[b], and Rainer Beckert[b]

[a] Institute of Inorganic and Analytical Chemistry, Friedrich Schiller University, Lessingstraße 8, D-07743 Jena, Germany
[b] Institute of Organic and Macromolecular Chemistry, Friedrich Schiller University, Humboldtstraße 10, D-07743 Jena, Germany

Reprint requests to Prof. Dr. D. Walther or Prof. Dr. R. Beckert. E-mail: Dirk.Walther@uni-jena.de, fax: (+49) (0)3641948172 or E-mail: Rainer.Beckert@uni-jena.de, fax: (+49) (0)3641948212.

Z. Naturforsch. **60b,** 843 – 852 (2005); received May 27, 2005

The reaction of the 2,3-dianilino-quinoxaline **1** with an equivalent of triethyl orthoformiate results in a cyclic aminalester **2**. An excess of triethyl orthoformate results in the carbene dimer **4**. With the help of boron trifluoride, **2** can be transformed into the imidazolium salt **3**. Reaction of **1** with $KOtC_4H_9$ leads to a quinoxaline derivative **5** under anellation of a benzene ring whereas the related pyrazino-quinoxaline **6** (formed from tetraaminobenzene tetrahydrochloride and bis-(3-trifluoromethylphenyl) oxalimidoyl chloride) does not react under similar conditions. However, **6** can be activated towards anellation by employing the complex fragment $[(tbbpy)_2Ru]^{2+}$, tbbpy: bis(4,4'-di-*tert*-butyl-2,2'-bipyridine). This generates an unusual ruthenium complex **9** which could be characterised by X-ray diffraction. Complex **9** contains a pentacene derivative and coordinates the ruthenium fragment at the amidinate moiety thus forming a four-membered chelate ring. Isolation of a second ruthenium complex **8** which contains an intact pyrazino-quinoxaline **6** in which the metal is also coordinated to an amidinato group supports the assumption that the anellation reaction occurs only after metal complexation at the amidinate group. In contrast to this, the smaller $[(tmeda)_2Pd]^{2+}$ fragment reacts with the pyrazino-quinoxaline **6** to form the mononuclear Pd complex **10**. Its structural motif (X-ray diffraction) shows that the palladium centre coordinates at the 1,4-diamino group of the intact pyrazino-quinoxaline to form a five-membered chelate ring. This suggests that the bulkiness of the complex fragment determines whether or not an anellation reaction can take place.

Key words: Diamino-Substituted Pyrazino-Quinoxalines, Annelation Reactions, Ruthenium Amidinate Complexes

Introduction

We have recently reported that the trifluoromethyl-substituted bisimidoyl chloride of oxalic acid undergoes cascade reactions to form azaquinones [1], 4*H*-imidazoles [2] and tetraazafulvalenes [3]. Furthermore, cyclisation of ortho-phenylenediamines with oxalic bisimidoylchlorides led to 2,3-di anilino-quinoxalines **1** which have been demonstrated to be a new class of tuberculostatics [4].

In this paper we continue our work by showing that easily accessible vicinal diamines of type **1** (Scheme 1) can be used as new synthetic building blocks for both cyclisations and intramolecular nucleophilic substitution reactions (anellations) of aromatic compounds.

When employing the related pyrazino-quinoxalines (type **6**), these anellations do not take place under typical (strong basic) anellation conditions. The synthetic protocol for the cyclisation of compound **1** to form the product **5** was adopted upon **6** but no reaction did occur.

The anellation can, however, be induced *via* complexation of **6** with a complex metal fragment $[(tbbbipy)_2Ru]^{2+}$. In contrast to this, the quite a bit smaller complex fragment $[(tmeda)_2Pd]^{2+}$ cannot activate this anellation. Solid state structures of these metal complexes give mechanistic indications of how these anellations take place, which we discuss in this article.

Results and Discussion

Reaction of diaminosubstituted quinoxalines

Diamino-substituted quinoxalines **1** are typical representatives of vicinal diamines and, as such, are often

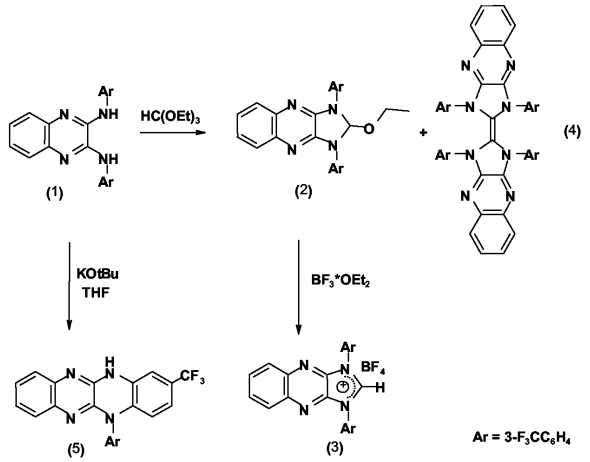

Scheme 1. Ring closure reactions of diaminosubstituted quinoxalines.

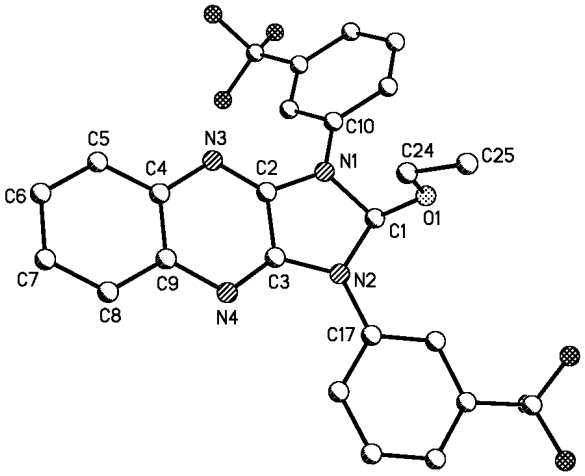

Fig. 1. Molecular structure of the aminal ester **2**. Selected bond distances (Å) and bond angles (deg): O1-C1 1.400(4), O1C24 1.439(4), N1-C1 1.456(4), N1-C10 1.417(4), N1-C2 1.374(4), N2-C1 1.462(4), N2-C3 1.381(4), N3-C2 1.290(4), N3-C4 1.388(4), N4-C3 1.295(4), C2-C3 1.444(4); C1-O1-C24 115.1(2), O1-C1-N1 114.0(2), O1-C1-N2 112.6(2), N1-C1-N2 102.9(2), C2-N1-C1 110.6(2), C3-N2-C1 110.4(2), N2-C3-C2 107.4(2), N4-C3-N2 129.2(2).

employed as interesting chemical precursors for further reactions [5].

We consider some of these reactions in this publication (Scheme 1).

If one employs Wanzlick's method (used for generating carbene precursors), the derivatives **1** can be cyclized with triethyl orthoformiate to yield cyclic aminalesters of type **2**. Compounds **2** exhibit an intensive blue fluorescence.

Encouraged by the progress reported for the chemistry of nucleophilic carbenes in the past few years, we thought it should be feasible to transform compounds **2** into carbenes. As a first step to this end, we succeeded in transforming the aminal esters **2** into their corresponding imidazolium salts. Boron trifluoride proved to be the reagent of choice as it reacts smoothly with the derivatives **2** to yield salts of type **3** in good yields (75%).

Elemental analyses as well as the sharp singlet observed at $\delta = 7.37$ ppm in the ^{1}H NMR spectra of **3** support the structural assignment of an imidazolium salt. Unfortunately, as soon as the salts are dissolved in alcohols, the aminalesters **2** are recovered. We succeeded in crystallising the methyl **2** and ethyl **2'** derivatives from a methanol/ethanol (1:1) mixture. The solid state structure of the methyl derivative **2** crystallizing with both 0,5 mol CH_3OH and 0,5 mol C_2H_5OH is illustrated in Fig. 1. Several attempts to generate stable carbenes – or their dimers – by employing strong bases such as NaH or alkoxides were unsuccessful.

However, if one heats an aminalester **2** in an excess of orthoformiate, the solution turns ruby-red and the carbene-dimer **4** can be isolated in a good yield. Compound **4** is a ring-fused tetraaminoethylene which is stable towards air and moisture. In addition, it exhibits a remarkably bathochromic UV/vis absorption at $\lambda_{max} = 551$ nm $(\log \varepsilon = 4.6)$ which corresponds to a shift of about 180 nm as compared to the starting product **2**.

We then attempted to obtain further quinoxaline derivatives with interesting physical properties by refluxing **1** for several hours in in the presence of a strong base ($KOtC_4H_9$). In this manner we succeeded in obtaining the fluorescent product **5** which could be isolated. The NMR spectrum of the main product (20% yield) indicated that one aromatic hydrogen had been lost. Solid state X-ray diffraction (see Experimental Section) confirmed that a ring fusion reaction had taken place and compound **5** (Scheme 1) had been formed. This is a rare example of a nucleophilic aromatic substitution of hydrogen (NASH) which resulted in anellation of the benzene ring. Usually only nitroaromatic compounds are known to undergo such reactions [6]. The reaction was carried out under natural atmospheric conditions and oxidation of the σ^H-adduct formed by air oxygen is likely to have occurred. We confirmed this by bubbling O_2 into the solution – which resulted in an increase of *ca.* 10% in the final yield of **5**.

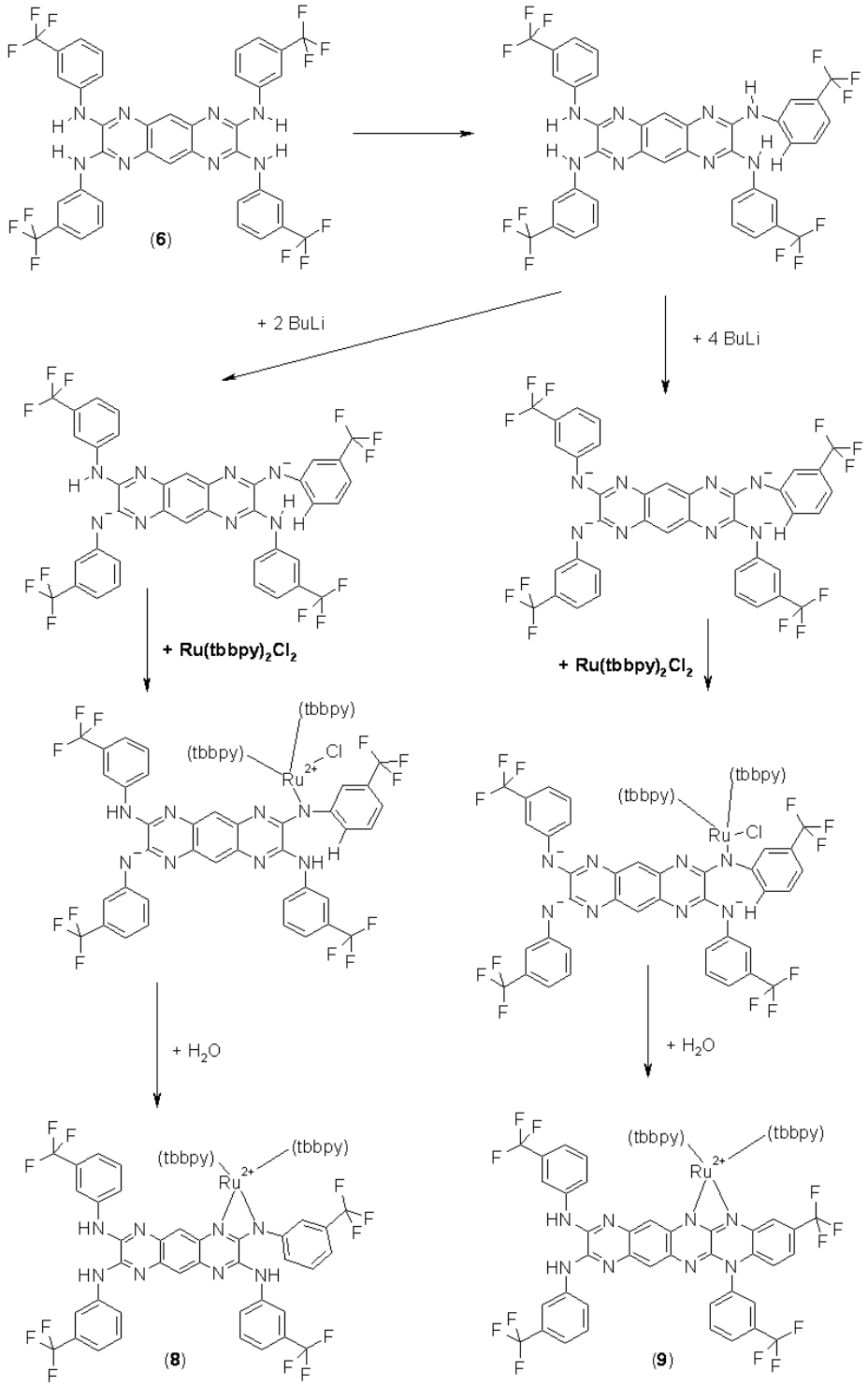

Scheme 2. Suggested possible reaction pathway for the formation of **8** and **9**.

Reactions of pyrazino-quinoxalines

The pyrazino-quinoxaline **6** (Scheme 2) could be synthesized by refluxing a mixture of tetraaminobenzene- tetrahydrochloride and bis-(3-trifluoromethylphenyl)-oxalimidoylchloride in acetonitrile [7]. The ^{1}H NMR spectrum of **6** in THF-D_8 shows several proton signals which suggests that different tautomers are present. In particular, the NH protons show three pairs of independent signals. Two singlets are found with equal intensities at $\delta = 9.52$ and 10.02 ppm. A second pair of singlets (9.48 and 9.92 ppm) are only 10% as intensive as the first pair. The third pair of singlets appears at 9.40 and 8.97 ppm and are 5% as intensive as the first pair. The aromatic protons also exhibit a complex pattern of signals (see Experimental Section). In contrast to this, the ^{1}H NMR spectrum of **6** in DMSO-D_6 shows a very simple pattern which suggests the presence of only one tautomer with a highly symmetrical structure. Only one signal for the NH protons ($\delta = 9.33$ ppm) is observed. Three, well separated aromatic proton signal groups at $\delta = 7.38$ (d, $J = 7.2$ Hz, 4H); 7.61 (t, $J = 8.0$ Hz, 4H) and 8.26 (d, $J = 7.6$ Hz, 4H) ppm can clearly be assigned to the *meta* protons in the aromatic rings. Furthermore, two singlets at $\delta = 7.64$ and 8.32 ppm can be assigned to the protons sitting next to the CF_3-groups and to the proton at the central phenyl ring. ^{1}H-decoupled ^{19}F NMR spectra which exhibit a single signal at $\delta = -61.76$ ppm confirm the presence of only one symmetrical compound in DMSO-D_6. Thus, compound **6** exists as a symmetrical heterotricyclic compound possessing two peripheral 3-CF_3-anilino groups on each side in DMSO solutions.

The solid state structure of **6** determined by single crystal X-Ray crystallography shows a symmetrical structure as well, which corresponds well to the ^{1}H NMR signal pattern found in DMSO (Fig. 2). Compound **6** crystallizes together with two molecules of DMSO which are hydrogen-bonded to the peripheral 1,4-diamino groups. All bond distances lie in the expected range.

Symmetry transformations used to generate equivalent atoms: A: $-x+2, -y+2, -z$.

Compound **6** reacts almost quantitatively with triethyl orthoformate to form the strongly fluorescent *bis*-aminalester **7**. In analogy to **1**, the pyrazino-quinoxaline **6** should be able to undergo ring closure reactions upon deprotonation with four equivalents of either butyl lithium or potassium *tert*-butanolate. This

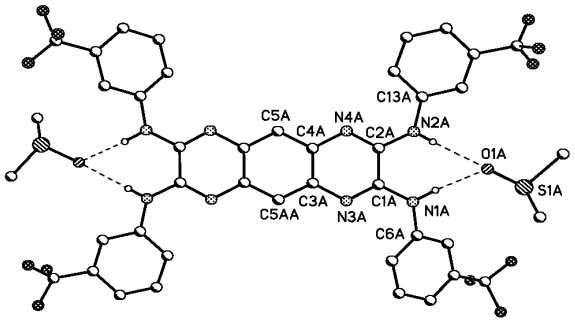

Fig. 2. Molecular structure of **6** as the adduct with two molecules of DMSO. Selected bond distances (Å) and bond angles (deg): N1A-O1A 2.882(5), N2A-O1A 2.915(5), N1A-C1A 1.375(5), N2A-C2A 1.377(5), N1A-C6A 1.409(6), N2A-C13A 1.399(6), N3A-C1A 1.306(5), N4A-C2A 1.301(5), N3A-C3A 1.376(5), N4A-C4A 1.385(5), C1A-C2A 1.469 (6), C3A-C4A 1.420(6), C3A-C5AA 1.396(6), C4A-C5A 1.391(6); C1A-N1A-C6A 125.9(4), C2A-N2A-C13A 130.1(4), C1A-N3A-C3A 117.9(4), C2A-N4A-C4A 117.6(4), N3A-C1A-N1A 118.9(4), N3A-C1A-C2A 121.2(4), N1A-C1A-C2A 119.9(4), C4A-C2A-N2A 119.4(4), N4A-C2A-C1A 121.7(4), N2A-C2A-C1A 118.9(4).

should result in single or double anellations under formation of novel aza-derivatives of pentacene or heptacene. Surprisingly, this reaction did not take place – even if a large excess of base (1:8 ratio) was employed. After refluxing **6** and the base in THF, only the starting compound could be recovered.

We then investigated whether the fully deprotonated **6** is able to act as a metal ligand by reacting it with a metallo-fragment $(tbbpy)_2RuCl_2$ [tbbpy: bis(4,4'-di-*tert*-butyl-2,2'-bipyridine]. This should result in either mono or dinuclear metallo complexes (depending on the ligand:metal molar ratio employed) in which the ligands form five-membered chelate rings at their peripheral 1,4-diaza coordination spheres. Such chelate complexes could possibly exhibit interesting photophysical properties. Furthermore, they might be suitable for photoactivated catalytic conversions.

If **6** (completely deprotonated) is refluxed with the ruthenium fragment (1:1 ratio) in dioxane/THF (1:2), the mononuclear ruthenium complex **9** can be isolated after column chromatographic purification. A possible path of formation of the ruthenium complexes **8** and **9** is depicted in Scheme 2. Mass spectrometric analysis of pure **9** using micro electron spray ionisation in methanol yielded a molecular peak at 1455.2 mmu which corresponds to a formula of $C_{74}H_{68}N_{12}F_{12}Ru$ (calculated mass is 1454.5 mmu). The calculated isotope pattern perfectly matches experiment. NMR spec-

tra indicate that the molecular structure of **6** is unsymmetrical because four different and well separated singlets occur in both ^{19}F- and ^{13}C-spectra (CF_3 and CH_3 groups).

Single crystals of **9**, suitable for an X-ray determination, were grown from a mixture of methanol and cyclohexane using diffusion methods. Under these conditions the complex crystallizes together with different solvent molecules (cyclohexane, triethylamine and methanol). Fig. 3 shows the solid state structure of **9**. The most interesting feature in **9** is that a pentacene derivative has been formed. The ruthenium moiety which coordinates at one side of the organic ligand has induced a ring closure reaction. In the absence of the transition metal ion, this does not occur. Furthermore, it is remarkable that the ruthenium fragment did not coordinate at the free 1,4-diamino group to form a five-membered chelate ring. Instead, the ruthenium coordinates in a rather untypical mode at the amidinate group to form a four-membered chelate ring. Although simple ruthenium complexes containing amidinate ligands have been well described [8 – 16], the existence of (polypyridyl)$_n$Ru(amidinate) complexes is, to our knowledge, yet unknown. Furthermore, it is somewhat surprising that the amidinate coordination in **9** is favored over the formation of a five-membered chelate ring *via* the 1,4-diamino group.

The π-electron system in **9** is completely conjugated as can be inferred from the bond distances and angles (Fig. 3). The ruthenium centre is symmetrically bound to the amidinate resulting in almost the same bond distances C(1)-N(1) (1.334(5) Å) and C(1)-N(3) (1.326(5) Å) within the experimental error. In addition, the bond lenghts Ru-N(1) (2.104(4) Å and Ru-N(2) (2.123(3) Å are not much different. This obviously results from a partial oxidation reaction during the formation of the complex. Thus the bond distances of C(16)-N(2) (1.423(6) Å) and C(5)-N(5) (1.376(6) Å) are comparable amongst each other and are significantly longer than the bond distances C(2)-N(4) (1.309(5) Å) and C(10)-N(6) (1.297(6) Å). The same result was found by comparing the bond distances of C(6)-N(6) (1.376(5) Å) and C(9)-N(5) (1.323(5) Å). NMR investigations confirm that the solid state structure is also present in solution (THF-D_8). Four different signals are found in the ^{19}F-NMR spectrum which supports an unsymmetrical structure assignment for **9**. The appearance of four different *t*-butyl signals in both the ^{1}H and ^{13}C NMR also indicate an unsymmetrical coordination environment of the

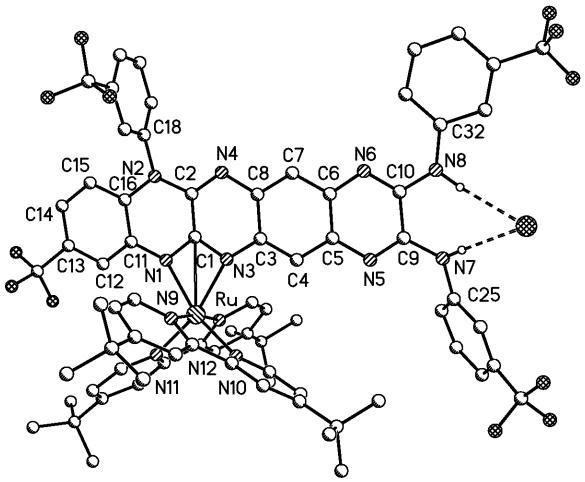

Fig. 3. X-ray crystal structure of the ruthenium complex **9** (solvent molecules in the crystal are omitted for clarity). Selected bond distances (Å) and bond angles (°): Ru-N9 2.056(4), Ru-N10 2.043(4), Ru-N11 2.052(3), Ru-N12 2.036(4), Ru-N1 2.104(4), Ru-N3 2.123(3), Ru-C1 2.548(4), N1-C11 1.382(6), N2-C16 1.423(6), N2-C18 1.459(6), N1-C1 1.334(5), N2-C2 1.378(5), N3-C1 1.326(5), N3-C3 1.381(5), N4-C2 1.309(5), N4-C8 1.390(5), N5-C5 1.376(6), N5-C9 1.323(5), N6-C6 1.376(5), N6-C10 1.297(6), N7-C9 1.361(6), N8-C10 1.380(5), C1-C2 1.433(6), C3-C4 1.383(6), C3-C8 1.439(6), C4-C5 1.405(6), C5-C6 1.412(6), C6-C7 1.391(6), C7-C8 1.399(6), C9-C10 1.467(6), C11-C12 1.377(6), C11-C16 1.425(6), C12-C13 1.398(7), C13-C14 1.371(8); N12-Ru-N10 95.41(14), N12-Ru-N11 78.21(14), N10-Ru-N11 98.75(14), N12-Ru-N9 171.53(14), N10-Ru-N9 78.60(14), N11-Ru-N9 96.65(14), N12-Ru-N1 93.11(14), N10-Ru-N1 160.78(13), N11-Ru-N1 99.85(14), N9-Ru-N1 94.41(15), N12-Ru-N3 97.17(13), N10-Ru-N3 99.06(13), N12-Ru-C1 98.15(14), N11-Ru-C1 131.37(14), N10-Ru-C1 129.73(13), N9-Ru-C1 90.30(14), N1-Ru-N3 62.72(13), N1-Ru-C1 31.53(13), N3-Ru-C1 31.32(13), C1-N1-C11 118.2(4), C1-N1-Ru 92.9(3), C1-N3-Ru 92.3(2).

metal centre. In addition, the experimental ESI mass spectrum completely matches the calculated isotope pattern of $C_{74}H_{68}N_{12}F_{12}Ru$.

A similar mononuclear ruthenium complex **8** can be obtained when $(tbbpy)_2RuCl_2$ is reacted with a doubly deprotonated **6** (note that fully deprotonated **6** is needed to obtain **9**). After chromatographic work up, crystals of complex **8** were isolated. Their insufficient quality, however, did not allow a fully resolved solid state structure to be obtained. The structural motif presented in Fig. 4 could, however, be deduced from the data. It is clear that the ruthenium atom is coordinated in the same mode as observed in **9**.

The most important difference between **8** and **9** is that the ring closure reaction to form the pentacene did

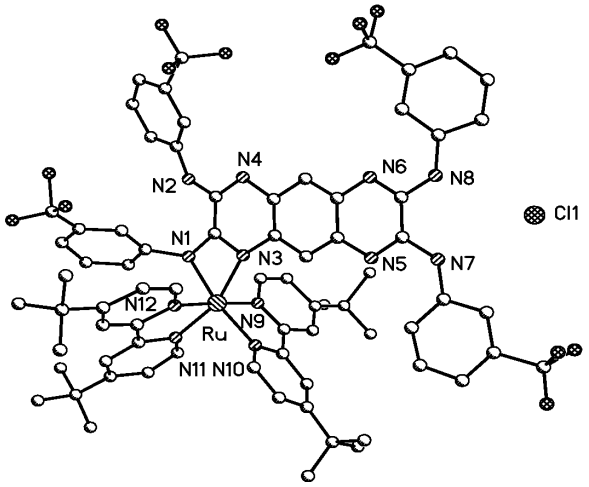

Fig. 4. Structural motif of the ruthenium complex **8**.

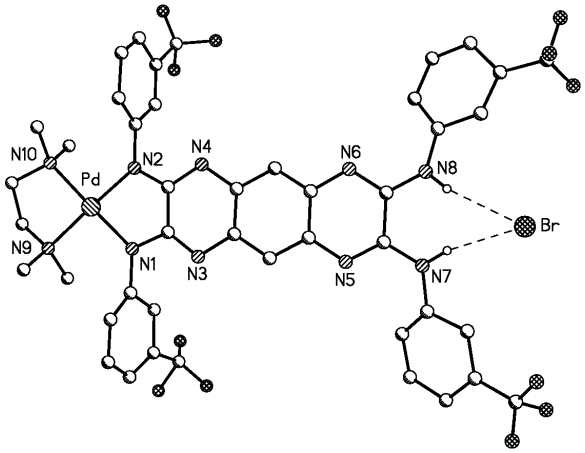

Fig. 5. Structural motif of the palladium complex **10**. (The anion $[(tmeda)(LiCl_2]^-$ and all solvent molecules in the crystal are omitted for clarity).

not occur in **8**. Thus **8** can be understood as an intermediate along the reaction pathway to the pentacene derivative **9**.

A possible route for the formation of **8** and **9** from **6** is illustrated in Scheme 2. In the first step, the ruthenium fragment attacks one peripheral amino function (N(1)). Since the $(tbbpy)_2Ru$ fragment is rather bulky, it cannot subsequently coordinate to N(2) due to steric hinderance. Formation of the usually energetically favored five-membered chelate ring is thus slowed down or completely stopped. Competitive coordination to N(3) to generate a four membered chelate ring then becomes the preferred reaction pathway. As the ring is formed, the aryl group bound to N(1) rotates toward the N(2) atom. This structure was found in complex **8** whereby N(2) is still protonated. If N(2) is deprotonated, the subsequent ring closure reaction to form the pentacene derivative **9** is facilitated.

This mechanism is supported by the different course of the reaction when the smaller metallo fragment (tmeda)Pd(II) is employed (with the completely deprotonated ligand **6**). In this case, the black Pd complex **10** was isolated in single crystals from commercially available solvents (dichloromethane and benzene). Due to insufficient quality of the single crystals obtained, only the structural motif of **10** in the solid state could be determined (Fig. 5). In contrast to both **8** and **9**, a five-membered chelate ring is formed using N(1) and N(2) as donor atoms in the Pd complex **10**. No anellation of the organic ligand was observed. We believe that this observation is due to the better 'fit' of the Pd-complex fragment into the 1,4-diamino coordination sphere as compared to the more bulky ruthenium fragments.

10 contains also a bromide ion bond at the peripheral NH bonds of the organic ligand. In addition, it contains also the anion $[(tmeda)LiCl_2]^-$ (omitted in Fig. 5 for clarity). Furthermore it contains also solvent molecules (see Experimental Section).

Conclusions

Our investigations show how subtle steric and electronic effects of differing metallo-fragments can drastically affect the coordination mode and the subsequent organic chemistry of 1,4-diamino substituted quinoxalines. We are currently utilising this knowledge for obtaining further interesting anellation reactions.

Experimental Section

Crystal structure determination for **2**, **5**, **6**, **8**, **9**, *and* **10**

The intensity data for the compounds were collected on a Nonius KappaCCD diffractometer, using graphite-monochromated Mo-K_α radiation. Data were corrected for Lorentz and polarization effects, but not for absorption effects [17, 18]. The structures were solved by direct methods (SHELXS [19]) and refined by full-matrix least squares techniques against F_o^2 (SHELXL-97 [20]). The hydrogen atoms of the amine group at N2 of **5** respectively N1 and N2 for **6** were located by difference Fourier synthesis and refined isotropically. All other hydrogen atoms were included at calculated positions with fixed thermal parameters. All non-hydrogen atoms were refined anisotropically [20]. The quality of the data of compounds **8** and **10** are too bad, hence

we will only publish the conformation of these molecules and the crystallographic data. We will not deposit these data in the Cambridge Crystallographic Data Centre. XP (SIEMENS Analytical X-ray Instruments, Inc.) was used for structure representations.

Crystal data for **2** [21]: $C_{23}H_{13}F_6N_4O \cdot 0.5\ CH_3OH \cdot 0.5\ C_2H_5OH$, $M_r = 497.42$ gmol^{-1}, colourless prism, size $0.10 \times 0.08 \times 0.06$ mm^3, monoclinic, space group $P2_1/c$, $a = 9.7016(2)$, $b = 12.8154(4)$, $c = 17.7951(5)$ Å, $\beta = 100.1860(1)^\circ$, $V = 2177.59(10)$ Å^3, $T = -90$ °C, $Z = 4$, $\rho_{calcd.} = 1.517$ g cm^{-3}, μ(Mo-K$_\alpha$) = 1.31 cm^{-1}, $F(000) = 1016$, 8216 reflections in $h(-12/12)$, $k(-16/15)$, $l(-23/23)$, measured in the range $2.13^\circ \leq \Theta \leq 27.46^\circ$, completeness $\Theta_{max} = 99.5\%$, 4970 independent reflections, $R_{int} = 0.028$, 3310 reflections with $F_o > 4\sigma(F_o)$, 317 parameters, 0 restraints, $R1_{obs} = 0.076$, $wR^2_{obs} = 0.206$, $R1_{all} = 0.113$, $wR^2_{all} = 0.233$, GOOF = 1.040, largest difference peak and hole: $1.154/-0.811$ e Å^{-3}.

Crystal data for **5** [21]: $C_{22}H_{12}F_6N_4$, $M_r = 446.36$ g mol^{-1}, colourless prism, size $0.04 \times 0.04 \times 0.03$ mm^3, monoclinic, space group $P2_1/n$, $a = 12.2272(2)$, $b = 4.9227(1)$, $c = 31.0849(6)$ Å, $\beta = 98.918(1)^\circ$, $V = 1848.41(6)$ Å^3, $T = 20$ °C, $Z = 4$, $\rho_{calcd.} = 1.604$ g cm^{-3}, μ(Mo-K$_\alpha$) = 1.4 cm^{-1}, $F(000) = 904$, 10696 reflections in $h(-14/15)$, $k(-4/6)$, $l(-40/38)$, measured in the range $3.37^\circ \leq \Theta \leq 27.49^\circ$, completeness $\Theta_{max} = 99.2\%$, 4215 independent reflections, $R_{int} = 0.029$, 3004 reflections with $F_o > 4\sigma(F_o)$, 347 parameters, 0 restraints, $R1_{obs} = 0.046$, $wR^2_{obs} = 0.123$, $R1_{all} = 0.070$, $wR^2_{all} = 0.137$, GOOF = 1.019, largest difference peak and hole: $0.219/-0.188$ e Å^{-3}.

Crystal data for **6** [21]: $C_{38}H_{22}F_{12}N_8 \cdot 2\ C_2H_6SO$, $M_r = 974.89$ g mol^{-1}, red-brown prism, size $0.04 \times 0.04 \times 0.03$ mm^3, triclinic, space group $P1$, $a = 8.0642(3)$, $b = 14.4369(8)$, $c = 20.0608(9)$ Å, $\alpha = 69.456(2)$, $\beta = 81.348(3)$, $\gamma = 77.194(3)^\circ$, $V = 2125.83(17)$ Å^3, $T = -90$ °C, $Z = 2$, $\rho_{calcd.} = 1.523$ g cm^{-3}, μ(Mo-K$_\alpha$) = 2.27 cm^{-1}, $F(000) = 996$, 13825 reflections in $h(-10/9)$, $k(-16/18)$, $l(-21/25)$, measured in the range $1.09^\circ \leq \Theta \leq 27.43^\circ$, completeness $\Theta_{max} = 95.5\%$, 9286 independent reflections, $R_{int} = 0.043$, 5996 reflections with $F_o > 4\sigma(F_o)$, 617 parameters, 0 restraints, $R1_{obs} = 0.101$, $wR^2_{obs} = 0.258$, $R1_{all} = 0.149$, $wR^2_{all} = 0.296$, GOOF = 1.012, largest difference peak and hole: $0.867/-0.907$ e Å^{-3}.

Crystal data for **8**: $C_{74}H_{69}Cl_2F_{12}N_{12}Ru \cdot 1/2\ CH_2Cl_2$, $M_r = 1533.40$ g mol^{-1}, red-brown prism, size $0.03 \times 0.03 \times 0.02$ mm^3, monoclinic, space group $P2_1/c$, $a = 15.7091(5)$, $b = 24.3356(5)$, $c = 21.1156(9)$ Å, $\beta = 91.590(1)^\circ$, $V = 8069.2(5)$ Å, $T = -90$ °C, $Z = 4$, $\rho_{calcd.} = 1.262$ g cm^{-3}, μ(Mo-K$_\alpha$) = 3.35 cm^{-1}, $F(000) = 3148$, 29129 reflections in $h(-20/20)$, $k(-30/25)$, $l(-27/27)$, measured in the range $2.31^\circ \leq \Theta \leq 27.46^\circ$, completeness $\Theta_{max} = 88.9\%$, 16434 independent reflections.

Crystal data for **9** [21]: $C_{74}H_{67}ClF_{12}N_{12}Ru \cdot 2.5\ C_6H_{12} \cdot 0.5\ N(C_2H_5)_3 \cdot 0.5\ CH_3OH \cdot 0.5\ H_2O$, $M_r = 1774.93$ g mol^{-1}, brown prism, size $0.03 \times 0.03 \times 0.02$ mm^3, monoclinic, space group $P2_1/c$, $a = 14.9151(5)$, $b = 32.5208(9)$, $c = 20.5356(7)$ Å, $\beta = 103.130(1)^\circ$, $V = 9700.4(5)$ Å^3, $T = -90$ °C, $Z = 4$, $\rho_{calcd.} = 1.215$ g cm^{-3}, μ(Mo-K$_\alpha$) = 2.62 cm^{-1}, $F(000) = 3708$, 34922 reflections in $h(-14/19)$, $k(-34/42)$, $l(-26/26)$, measured in the range $1.66^\circ \leq \Theta \leq 27.48^\circ$, completeness $\Theta_{max} = 91.3\%$, 20298 independent reflections, $R_{int} = 0.051$, 14853 reflections with $F_o > 4\sigma(F_o)$, 1053 parameters, 0 restraints, $R1_{obs} = 0.079$, $wR^2_{obs} = 0.209$, $R1_{all} = 0.113$, $wR^2_{all} = 0.240$, GOOF = 1.107, largest difference peak and hole: $1.192/-0.702$ e Å^{-3}.

Crystal data for **10**: $C_{44}H_{38}BrF_{12}N_{10}Pd \cdot C_6H_{16}N_2Cl_2Li \cdot 3.5\ C_6H_6$, $M_r = 1586.56$ g mol^{-1}, colourless prism, size $0.03 \times 0.03 \times 0.02$ mm^3, monoclinic, space group $P2_1/n$, $a = 16.9412(4)$, $b = 17.0885(5)$, $c = 29.4685(9)$ Å, $\beta = 90.712(2)^\circ$, $V = 8530.5(4)$ Å^3, $T = -90$ °C, $Z = 4$, $\rho_{calcd.} = 1.235$ g cm^{-3}, μ(Mo-K$_\alpha$) = 8.17 cm^{-1}, $F(000) = 3236$, 34149 reflections in $h(-21/20)$, $k(-22/21)$, $l(-38/29)$, measured in the range $2.38^\circ \leq \Theta \leq 27.48^\circ$, completeness $\Theta_{max} = 89.9\%$, 17566 independent reflections.

*2-Ethoxy-1,3-bis(3-(trifluoromethyl)phenyl)-1,3-dihydro-1H-imidazo[4,5-b]quinoxaline (**2**)*

A mixture of 200 mg (0.44 mmol) of 2,3-bis-(3-trifluoromethylanilino)quinoxaline and 25 ml of triethyl orthoformate was refluxed for about 5 h under soft argon stream. After removal of the excessive orthoformiate by distillation the crude product was purified by column chromatography (Al_2O_3, toluene/acetone : 10/1).

Yellowish crystals; m. p. = 189 – 191 °C; 80% yield. – MS (neg. CI with H_2O); *m/z* (%) = 504 (100) [M$^-$]. – ^{1}H NMR (CD_2Cl_2): $\delta = 1.04$ (t, $J = 6.7$ Hz, 3 H), 3.29 (q, $J = 7.1$ Hz, 2 H), $\delta = 7.21$ (d, $J = 8.2$ Hz, 2 H), 7.22 (s, 1 H), 7.44 (dd, 2 H), 7.45 (m, 2 H), 7.76 (m, 2 H), 8.14 (d, $J = 8.2$ Hz, 2 H), 8.37 (s, 2 H). – ^{13}C NMR (CD_2Cl_2): $\delta = 14.60$, 56.03, 95.58, 117.21 (q, ^3J (C,F) = 3.8 Hz), 119.19 (q, J (C,F) = 3.8 Hz), 124.75 (q, J (C,F) = 272.3 Hz), 126.63, 127.13, 130.64, 131.83 (q, ^2J (C,F) = 32.0 Hz), 137.45, 139.12, 143.41. UV/vis (DMSO): $\lambda_{max}(\varepsilon) = 274$ (4.5), 325 (4.0), 341 (4.2), 357 (4.4), 375 (4.3). – $C_{25}H_{18}F_6N_4O$ ($M_r = 504.43$ g mol^{-1}): calcd. C 59.53, H 3.60, N 11.11; found C 59.62, H 3.68, N 11.05.

*1,3-Di(3-(trifluoromethyl)phenyl)-2-(1,3-di(3-trifluoromethyl)phenyl)-2,3-dihydro-1H-imidazo[4,5-b]quinoxaline-2-ylidene)-2,3-dihydro-1h-imidazo[4,5-b]quinoxalin (**4**)*

Analogous to **2** except of the prolonged time of reaction of 24 h; red crystals m. p. = 211 – 213 °C (dec.); yield 62%. –

MS (CI with H_2O): *m/z* (%) = 313 (65), 474 (100), 916 (25) (M^+). – ^{1}H NMR (CD_2Cl_2): $\delta = 7.39$ (m, 4 H), 7.42 (s, 4 H), 7.43 (d, $J = 8.2$ Hz, 4 H), 7.45 (m, 4 H), 7.51 (d, $J = 8.2$ Hz, 4 H), 7.62 (m, 4 H). – ^{13}C NMR (CD_2Cl_2): 112.59, 122.17 (q, ^3J (C,F) = 3.8 Hz), 123.42, 123.89 (q, ^1J (C,F) = 273.3 Hz), 126.86, 127.29, 127.42, 129.43, 131.13 (q, ^2J (C,F) = 32.0 Hz), 136.12, 139.06, 144.15. – UV/vis (DMSO): $\lambda_{max}(\varepsilon) = 345$ nm (4.1), 485 (4.5), 514 (4.6), 551 (4.3). – C_{46} $H_{24}F_{12}N_8$ ($M_r = 916.19$ g mol^{-1}): calcd. C 60.27, H 2.64, N 12.22; found C 60.47, H 2.68, N 12.05.

*1,3-Bis-(3-trifluoromethyl-phenyl)-3H-imidazo[4,5-b]quinoxalin-1-ium (**3**)*

To a solution of 0.1 g of **5** in 10 ml of THF BF_3-etherate (0.1 ml) was added in drops. After stirring at room temperature for 1 h, half of the solvent is removed by evaporation. The precipitated colorless crystals were filtered and washed with dichloromethane.

Colorless crystals: m. p. = 220 – 222 °C (dec.); yield 75%. – MS (DCI with H_2O): *m/z* (%) = 257 (60), 281 (50), 439 (20) (M^+-F), 459 (100) (M^+), 479 (25) (M^++F). – ^{1}H NMR (CD_2Cl_2): $\delta = 7.37$ (s, 1 H), 7.49 (m, 2 H), 7.58 (d, $J = 7.79$ Hz, 2 H), 7.70 (d, $J = 8.10$ Hz, 2 H), 7.76 (m, 2 H), 8.45 (d, $J = 8.19$ Hz, 2 H), 8.53 (s, 1 H). – ^{13}C NMR (CD_2Cl_2): $\delta = 94.01$, 117.52 (q), 121.99 (q), 124.13, 126.68, 127.08, 130.67, 132.01 (q), 136.45, 138.47, 143.73. – UV/vis (DMSO): $\lambda_{max}(\varepsilon) = 324$ (3.9), 340 (4.0), 357 (4.1), 375 (4.0).

*2-Trifluoromethyl-5-(3-trifluoromethyl-phenyl)-5,12-dihydro-quinoxalino[2,3-b]quinoxaline (**5**)*

A mixture of quinoxaline **1**, potassium *t*-butylate and THF is refluxed and stirred for 16 h. After evaporation of the solvent the crude product is purified by column chromatography (SiO_2, toluene).

Yellow crystals, m. p. > 250 °C. yield 22%. – MS (DCI with H_2O): *m/z* (%) = 391 (75), 427 (100), 446 (80) (M^+). ^{1}H NMR (CD_2Cl_2): $\delta = 5.99$ (d, $J = 8.53$ Hz, 1 H), 6.76 (s, 1 H), 6.82 (d, $J = 8.53$ Hz, 1 H), 7.13 (m, 3 H), 7.25 (d, $J = 7.54$ Hz, 1 H), 7.61 (d, $J = 7.54$ Hz, 1 H), 7.68 (s, 1 H), 7.81 (m, 2 H). – $C_{22}H_{12}F_6N_4O$ ($M_r = 446.09$ g mol^{-1}): calcd. C 59.20, H 2.71, N 12.55; found C 59.41, H 2.81, N 12.36.

*N,N',N'',N'''-Tetrakis-(3-(trifluoromethyl)phenyl)pyrazino[2,3-g]quinoxaline-2,3,7,8-tetraamine (**6**)*

12.7 g (30.9 mmol) of the bisimidoylchloride was dissolved in 200 ml acetonitrile and 4.4 g (15.4 mmol) of 1,2,4,5-tetraaminobenzoltetrahydrochloride followed by treatment with 12.5 g (123.7 mmol) of triethylamine. The mixture was refluxed for 8 h and the solvent is evaporated afterward. Then the brown resin was washed twice with 50 ml *n*-heptane to remove unreacted bis(imidoyl chloride). The residue was put into 100 ml of water and the mixture was extracted with 2 × 100 ml dichloromethane. The organic phase was then washed with 2 × 80 ml water and dried over Na_2SO_4. Upon evaporation of the solvent the brown solid was dissolved in 200 ml methanol and treated with 10 ml toluene and 80 ml water. The resulting bright yellow amorphous solid was filtrated and dried *in vacuo*. A part of the product was dissolved in methanol. Reaction with hydrochloric acid yielded the crystalline triethylamine hydrochloride which crystallized in yellow single crystals. Additionally, from a saturated DMSO solution single crystals of the DMSO adduct could be isolated as yellow to brownish crystals.

MS (DCI in water): *m/z*= 819 ($(M+H)^+$), 799 ($(M-F)^+$). – ^{1}H NMR (DMSO-D_6): $\delta = 7.38$ (d, 4H, $J = 7.2$ Hz), 7.61 (t, 4H, $J = 8.0$ Hz), 7.64 (s, 2H), 8.26 (d, 4H, $J = 7.6$ Hz), 8.32 (s, 4H), 9.33 (s, 4H, NH). – ^{19}F NMR (DMSO-D_6) ^{1}H-decoupled $\delta = -61.68$ (s). – ^{13}C NMR 50 °C (DMSO-D_6) $\delta = 116.2$, 118.5, 119.0, 123.5, 124.1 (q, CF_3, $J = 272.2$ Hz), 129.3 (q, C-CF_3, $J = 31.7$ Hz), 129.6, 134.8, 140.8 (br, 2 signals). – ^{1}H NMR (THF-D_8, 600 MHz): $\delta = 7.26$ (s), 7.36 (m), 7.42 (s), 7.45 (d, $J = 8.5$ Hz); 7.50 (t, $^3J = 7.9$ Hz), 7.59 (m), 7.81 (s), 7.86 (d, $J = 7.3$ Hz), 7.95 (s), 8.07 (s), 8.17 (s), 8.36 (d, $J = 8.6$ Hz), 8.39 (d, $J = 8.6$ Hz); 8.50 (s), 8.54 (s), 8.60 (d, $J = 9.8$ Hz), 8.64 (s), 8.97 (s, NH), 9.40 (s, NH), 9.48 (s, NH), 9.52 (s, NH), 9.92 (s, NH), 10.02 (s, NH). – ^{19}F NMR (THF-D_8), ^{1}H-decoupled $\delta = -65.75$ (s), -65.74 (s), -65.66 (s), -65.67 (s). – $C_{38}H_{24}N_8F_{12}O$ ($M_r = 719$,(M·H_2O) calcd. C 54.55, H 2.89, N 13.40; found C 54.14, H 2.90, N 13.29.

*2,8-Diethoxy-1,3,7,9-tetrakis-(3-trifluoromethyl-phenyl)-1,2,3,7,8,9-hexahydro-1,3,4,6,7,9,10,12-octaaza-dicyclopenta[b,i]anthracene (**7**)*

Analogous to **2** from **6**; yellowish crystals m. p. > 250 °C (dec.). – MS (CI with H_2O): 930 (100) (M^+). – ^{1}H NMR (THF-D_8): $\delta = 1.01$ (t, $J = 7.0$ Hz, 6 H), 3.39 (q, $J = 7.0$ Hz, 4 H), 7.56 (d, $J = 7.75$ Hz, 4 H), 7.73 (dd, $J = 7.98$ Hz, 4 H), 7.90 (s, 2 H), 8.11 (s, 2 H), 8.75 (d, $J = 8.31$ Hz, 4 H), 8.82 (s, 4 H). – ^{13}C-NMR (THF-D_8): $\delta = 14.62$, 56.28, 95.90, 116.25 (q, ^3J (C,F) = 4.0 Hz), 121.27 (q, ^3J (C,F) = 3.8 Hz), 123.08, 125.22 (q, ^1J (C,F) = 272.3 Hz), 130.61, 131.91 (q, ^2J (C,F) = 32.2 Hz), 136.71, 139.28, 144.33. – UV/vis (DMSO): $\lambda_{max}(\varepsilon) = 293$ (4.7), 373 (3.9), 392 (4.3), 415 (4.6), 441 (4.7).

Complex **8**

In an argon atmosphere, 643 mg (786 μmol) of **6** were dissolved in a mixture of 1,4-dioxane and THF (1:2, 30 ml) and treated at −40 °C with 1.15 ml (1.56 mmol) of a butyllithium solution in hexane (1.36 molar) for 1 h under stirring. The ruby solution was allowed to warm up to room temperature and 650 mg (786 μmol) of $Ru(tbbpy)_2Cl_2$ were added. Refluxing the mixture for 8 h and evaporation of

the solvent resulted in a dark brown solid which was purified by chromatography on silica gel with a mixture of acetonitrile, dichloromethane and water (80:20:3). The second auburn band contained **8** which was crystallized from CH_2Cl_2/heptane.

^{1}H NMR (CD_2Cl_2): $\delta = 1.22$ (s, 9H, $(CH_3)_3$-), 1.33 (s, 9H,$(CH_3)_3$-), 1.38 (s, 9H, $(CH_3)_3$-); 1.44 (s, 9H,$(CH_3)_3$-), 6.17 (s, 1H), 6.24 (s,b, 1H), 6.28 (s,b, 2H), 6.56 (s, 1H), 6.91 (m, 1H), 7.00 (m, 1 H), 7.17 – 7.30 (m, 6 H); 7.40 (m, 2H); 7.44 (d, 2H, $J = 7.1$ Hz), 7.60 (dd, 1H, $J = 1.8$ Hz, $J = 6.0$ Hz), 7.76 (d, 1H, $J = 8.4$ Hz), 7.79 (d, 1H, $J = 9.2$ Hz), 7.91 (s, 2H), 7.96 (m, 2H), 8.03 (d, 1H, $J = 8.8$ Hz), 8.09 (s, 1H), 8.22 (s, 1H), 8.27 (s, 1H), 8.48 (d, 1H, $J = 6.0$ Hz), 8.65 (s, 1H), 9.16 (d, 1H, $J = 5.2$ Hz), 9.66 (s,b, 1H, NH), 9.81 (s,b, 1H, NH). – ^{19}F NMR (CD_2Cl_2), ^{1}H-decoupled $\delta = -63.56$ (s), -63.45 (s), -63.21 (s), -62.54 (s). – MS (Micro-ESI in methanol): *m/z* = 1455.4 mmu ($C_{74}H_{70}N_{12}F_{12}Ru^+$ = M-Cl^+). – UV/vis (methanol): $\lambda_{max} = 291$ (max. π-π^*-transition ligand), 437 (max. *n*-π^*-transition ligand), 497 (shoulder, ^{1}MLCT-transition complex).

Complex **9**

In an argon atmosphere, 404 mg (494 μmol) of **6** were dissolved in a mixture of 1,4-dioxane and THF (1:2, 40 ml) and treated at -40 °C with 1.42 ml (1.98 mmol) of a butyllithium solution in *n*-hexane (1.39 molar) for 1 h under stirring. The ruby solution was allowed to warm up to room temperature and 350 mg (494 μmol) of Ru(tbbpy)$_2$Cl$_2$ were added. The mixture was refluxed for 8 h and the solvent was evaporated afterward. The dark brown solid was purified by chromatography on silica gel with a mixture of chloroform, ethanol and triethylamine (20:4:1).

Alternatively **9** can be synthesized by the following pathway: 115.5 mg (141 μmol) of **6** and 14.3 μg (282 μmol, 19.6 μl) of triethylamine were dissolved in a mixture of ethanol and water (4:1). Upon addition of 100 mg (141 μmol) of Ru(tbbpy)$_2$Cl$_2$ the mixture was refluxed for 8 h followed by evaporation of the solvent. The dry crude product was washed with 3×20 ml of water and chromatographed on silica gel with a mixture of chloroform, ethanol and triethylamine (20:4:1) by means of a water cooled column. This was necessary to increase the separation ability of the chromatographic system. Compley **9** was eluted with the first auburn band which was crystallized from dichloromethane/benzene or methanol/cyclohexane.

^{1}H-NMR (CD_2Cl_2): $\delta = 1.22$ (s, 9H,$(CH_3)_3$-), 1.34 (s, 9H,$(CH_3)_3$-), 1.38 (s, 9H, $(CH_3)_3$-), 1.44 (s, 9H,$(CH_3)_3$-), 6.15 (s, 1H), 6.23 (s, 1H), 6.42 (s, 1H), 6.91 and 7.00 (m, 2H), 7.17 – 7.32 (m, 6H), 7.50 (d, 2H, $J = 5.6$ Hz), 6.61 (d, 2H, $J = 4.4$ Hz), 7.80 (d , 2H, $J = 8.4$ Hz), 7.90 – 7.98 (m, 4H), 8.09 (d, 2H, $J = 8.0$ Hz), 8.28 and 8.25 and 8.22 (m, 3H), 8.44 (d, 2H, $J = 8.4$ Hz), 8.48 (d, 2H, $J = 6$ Hz), 8.84 (s, 1H), 9.18 (d, 1H, $J = 6$ Hz), 10.32 (s, 1H, NH), 10.52 (s, 1H, NH). – ^{19}F NMR (CD_2Cl_2), ^{1}H-decoupled: $\delta = -63.58$ (s), -63.45 (s), -63.07 (s), -62.46 (s). – MS (Micro-ESI in methanol): *(m/z*= 1455.2 mmu ($C_{74}H_{70}N_{12}F_{12}Ru^+$ = M-Cl^+). – UV/vis (methanol): λ(nm) = 292 (max. π-π^*-transition ligand), 335 (shoulder *n*-π^*-transition bipyridine), 434 (max. *n*-π^*-transition ligand), 503 (shoulder, ^{1}MLCT-transition complex).

Complex **10**

300 mg (366 μmol) of **6** were dissolved in 50 ml dry THF and 0.91 ml (1.47 mmol) of a solution of butyllithium in hexane (1.6 molar) were added *via* a syringe at -78 °C. The solution was allowed to warm up to room temperature and under stirring 274 mg (732 μmol) Pd(cod)Br$_2$ in 25 ml THF and 1.1 ml (7.3 mmol) of dry tetramethylethylenediamine (tmeda) were added. Stirring of the mixture for 24 h at room temperature and distillation of the solvent in *vacuum* to dryness resulted in a dark brown solid which was washed twice with 20 ml dry *n*-hexane to remove redundant cod. The dry residue was dissolved in dichloromethane and filtrated on diatomite earth to remove lithium bromide. From the clear filtrate which was overlaid with benzene longish black crystals were obtained which were analyzed by X-ray diffraction analysis spectrometry. Hydrolysis of the complex might have occurred due to the use of non-dryed (commercially available) solvents in both mass spectroscopy and crystal formation. – MS (Micro-ESI in CH_2Cl_2 or 2-propanol) *(m/z* = 1039 ($C_{44}H_{37}N_{10}F_{12}Pd^+$ (M-H^+)).

Acknowledgements

Financial support of this work is gratefully acknowledged by the Deutsche Forschungsgemeinschaft (SFB 436), and the Fonds der Chemischen Industrie. We'd like to thank A. Malassa for support in the synthesis of the complex **10**.

[1] T. Billert, R. Beckert, P. Fehling, M. Döring, H. Görls, Tetrahedron **53**, 5455 (1997).
[2] J. Atzrodt, J. Brandenburg, C. Käpplinger, R. Beckert, W. Günther, H, Görls, J. Fabian, J. Prakt. Chem./Chemiker-Ztg. **339**, 729 (1997).
[3] C. Käpplinger, R. Beckert, W. Günther, H. Görls, Liebigs Ann./Recueil 617 (1997).
[4] R. Beckert, K. Waisser, D. Lindauer, C. Käpplinger, R. Walther, Pharmazie **52**, 638 (1997).
[5] E. Schipper, A. R. Day, J. Am. Chem. Soc. **73**, 5672 (1951).
[6] P. F. Pagoria, A. R. Mitchell, R. D. Schmidt, J. Org. Chem. **61**, 2934 (1996).
[7] C. Käpplinger, R. Beckert, Synlett **11**, 1679 (2000).

[8] H. Nagashima, H. Kondo, T. Hayashida, Y. Yamaguchi, M. Gondo, S. Masuda, K. Miyazaki, K. Matsubara, K. Kirchner, Coord. Chem. Rev. **245**, 177 (2003).
[9] T. Hayashida, K. iyazaki, Y. Yamaguchi, H. Nagashima, Journ. Organomet. Chem. **634**, 167 (2001).
[10] F. A. Cotton, T. Ren, Inorg. Chem. **30**, 3675 (1991).
[11] F.A . Cotton, T. Ren, Inorg. Chem. **34**, 3190 (1995).
[12] P. Angaridis, F. A. Cotton, C. A. Murillo, D. Villagrán, X. Wang, Inorg. Chem. **43**, 8290 (2004).
[13] L. D. Brown, S. D. Robinson, A. Sahajpal, J. A. Ibers, Inorg. Chem. **16**, 2728 (1977).
[14] S. D. Robinson, A. Sahajpal, J. Chem. Soc. Dalton Trans. 3349 (1997).
[15] T. Koizumi, T. Tomon, K. Tanaka, Bull. Chem. Soc. Jpn. **76**, 1969 (2003).
[16] H. Kondo, Y. Yamaguchi, H. Nagashima, Chem. Comm. **12**, 1075 (2000).
[17] COLLECT, Data Collection Software, Nonius B.V., The Netherlands (1998).
[18] Z. Otwinowski, W. Minor, in C. W. Carteer, R. M. Sweet (eds): Processing of X-Ray Diffraction Data Collected in Oscillation Mode, Methods in Enzymology, Macromolecular Crystallography, Part A, Vol. 276, pp. 307 – 326, Academic Press, London (1997).
[19] G. M. Sheldrick, Acta Crystallogr. Sect. A **46**, 467 (1990).
[20] G. M. Sheldrick, SHELXL-97 (Release 97-2), University of Göttingen, Germany (1997).
[21] CCDC 265916 (**2**), 265917 (**5**), 265918 (**6**), and 265919 (**9**) contains the supplementary crystallographic data for this paper. These data can be obtained free of charge *via* www.ccdc.cam.ac.uk/conts/retrieving.html (or from the Cambridge Crystallographic Data Centre, 12, Union Road, Cambridge CB2 1EZ, UK; fax: (+44) 1223-336-033; or deposit@ccdc.cam.ac.uk).